DEK modulates both expression and alternative splicing of cancer-related genes

BIN LIU, YUANLIN SUN, YANG ZHANG, YANPENG XING and JIAN SUO

Department of Gastrocolorectal Surgery, The First Hospital of Jilin University, Changchun, Jilin 130021, P.R. China

Received November 30, 2021; Accepted April 11, 2022

DOI: 10.3892/or.2022.8322

Abstract. DEK is known to be a potential proto-oncogene and is highly expressed in gastric cancer (GC); thus, DEK is considered to contribute to the malignant progression of GC. DEK is an RNA-binding protein involved in transcription, DNA repair, and selection of splicing sites during mRNA processing; however, its precise function remains elusive due to the lack of clarification of the overall profiles of gene transcription and post-transcriptional splicing that are regulated by DEK. We performed our original whole-genomic RNA-Seq data to analyze the global transcription and alternative splicing profiles in a human GC cell line by comparing DEK siRNA-treated and control conditions, dissecting both differential gene expression and potential alternative splicing events regulated by DEK. The siRNA-mediated knockdown of DEK in a GC cell line led to significant changes in gene expression of multiple cancer-related genes including both oncogenes and tumor suppressors. Moreover, it was revealed that DEK regulated a number of alternative splicing in genes which were significantly enriched in various cancer-related pathways including apoptosis and cell cycle processes. This study clarified for the first time that DEK has a regulatory effect on the alternative splicing, as well as on the expression, of numerous cancer-related genes, which is consistent with the role of DEK as a possible oncogene. Our results further expand the importance and feasibility of DEK as a clinical therapeutic target for human malignancies including GC.

Correspondence to: Dr Jian Suo or Dr Yanpeng Xing, Department of Gastrocolorectal Surgery, The First Hospital of Jilin University, 1 Xinmin Street, Chaoyang, Changchun, Jilin 130021, P.R. China
E-mail: suojian@jlu.edu.cn
E-mail: xingyanpeng@jlu.edu.cn

Abbreviations: A3SS & ES, alternative 3'splice site and exon skipping; A5SS & ES, alternative 5'splice site and exon skipping; ACTA2, alpha smooth muscle actin; APOBEC3H, apolipoprotein B mRNA editing enzyme catalytic subunit 3H; AS, alternative splicing; ASEs, alternative splicing events; ASNS, asparagine synthetase; CCDC80, coiled-coil domain containing 80; CDK11A, cyclin-dependent kinase 11A; CHAC1, cation transport regulator 1; CXCL10, chemokine (C-X-C motif) ligand 10; DDIT4, DNA damage-inducible transcript 4; DEG, differentially expressed gene; EPB41L1, erythrocyte membrane protein band 4.1 like 1; ERRFI1, ERBB receptor feedback inhibitor 1; FAM3C, FAM3 metabolism regulating signaling molecule C; FC, fold change; FDR, false discovery rate; GEO, Gene Expression Omnibus; GO, Gene Ontology; HMOX1, heme oxygenase-1; JDP2, Jun dimerization protein 2; KD, knockdown; KEGG, Kyoto Encyclopedia of Genes and Genomes; KIFC3, kinesin family member C3; MXEs, mutually exclusive exons; OSBPL5, oxysterol binding protein like 5; PDXDC1, pyridoxal-dependent decarboxylase domain-containing 1; PSAT1, phosphoserine aminotransferase 1; PSPH, phosphoserine phosphatase; RASEs, regulated alternative splicing events; RMRP, RNA component of mitochondrial RNA processing; RNA-Seq, RNA sequencing; RT-qPCR, quantitative reverse transcription-polymerase chain reaction; SAP, SAF-A/B, acinus and PIAS; SMEK1, SMEK homolog 1; SPRR2A, small proline-rich protein 2A; siCtrl, small interfering control; siDEK, small interfering DEK; siRNA, small interfering RNA; TCGA, The Cancer Genome Atlas

Key words: DEK, knockdown, RNA-seq, gene expression, alternative splicing, gastric cancer

Introduction

Gastric cancer (GC) is one among the foremost common malignant neoplasms within the digestive tract and is the fourth common malignancy and the third leading cause of cancer-related death worldwide (1,2). GC patients tend to be diagnosed at advanced stages, and the 5-year survival rate is no more than 40% in China (3). Although *Helicobacter pylori* has been reported as the most significant risk factor for GC (4), the exact etiology of GC is still unclear, and a detailed investigation of molecular mechanisms of GC is urgently needed to identify novel therapeutic and diagnostic targets. Cancer cells harbor a number of dysregulations in gene expression due to multiple aberrations in both transcription and splicing machinery and, at the same time, cancers are considered to rely on such abnormal homeostasis of gene expression networks for their survival. Thus, the importance of the clarification of spectrums of gene expression and alternative splicing in cancer cells, as well as the identification of potential master regulators of such transcriptional networks are warranted (5).

The DEK proto-oncogene (DEK) protein was identified as a fusion gene with nucleoporin 214 in a subset of patients with acute myeloid leukemia (6,7). Literature findings suggest that chromosomal aberrations at the DEK locus are also associated with the occurrence of human solid tumors (8,9). DEK has two

DNA binding modules, one of which is an SAP box, a domain that DEK shares with some other chromatin proteins. DEK plays a key role in various cellular processes and is involved in multiple genomic pathways, for example, global heterochromatin integrity (10), transcriptional regulation (11), mRNA splicing (12,13), DNA binding (14), DNA replication (15), DNA damage response, and repair (16). It has no apparent affinity to specific DNA sequences, but preferentially binds to superhelical and cruciform DNA, and induces positive supercoils into closed circular DNA; meanwhile, DEK participates in the selection of splicing sites during mRNA processing (17). Alternative splicing is one of the key molecular mechanisms which contribute to the biologically functional complexity of the human genome (18). It was reported that transcripts from ~95% of multiexon genes had alternatively spliced variants and in major human tissues (19). Noncanonical and cancer-specific mRNA transcripts produced by aberrant splicing can lead to loss of function of tumor suppressors or gain of function of oncogenes (20); thus, alternative splicing events play a pivotal role in carcinogenesis. According to a report, in addition to the regulation of splicing events, DEK is a candidate factor that also controls post-splicing steps in gene expression (12). The involvement of DEK in splicing has been reported. DEK is a factor that interacts *in vitro* and *in vivo* with SR proteins involved in pre-mRNA splicing and forms a splicing-dependent interaction with exon-product complexes (12); intron removal requires proofreading of the U2AF/3'splice site recognition by DEK (13); and DEK also acts on the proofreading of the 3'splice site (21). In view of the biological function, DEK is known to suppress cellular senescence, apoptosis, and differentiation, and thus promotes cell growth and survival (22). Importantly, DEK is also known to play a role in chronic inflammation and subsequent tumorigenesis by affecting nuclear factor (NF)-κB signaling (23). High expression of DEK in GC has been reported; furthermore, such overexpression of DEK was found to be related to a worse prognosis of GC patients (24-26); thus, DEK may be able to be used as a potential diagnostic marker for GC. In GC cell lines, DEK can promote cell migration and invasion (27-29), although the precise molecular mechanisms remain elusive. Taken together, DEK is considered an important oncogene in gastric carcinogenesis; however, its molecular function, more specifically its oncogenic function, as a regulator of gene expression and splicing events has not been investigated on a whole-genome scale to date. Therefore, it is urgent to clarify the effects of DEK on the overall gene transcription and post-transcriptional splicing in GC cells. The present study reveals a global picture of gene expression and splicing profiles as well as functional pathways that are regulated by DEK in a GC cell line and shows that DEK can transcriptionally affect multiple cancer-related signaling pathways.

Materials and methods

Cell culture and transfections. Human GC cell line AGS (Procell Life Science & Technology Co., Ltd., China) was cultured at 37˚C with 5% CO_2 in Ham's F-12 with 100 μg/ml streptomycin, 100 U/ml penicillin, and 10% fetal bovine serum (FBS). Human GC cell lines MKN1 and NUGC4 derived from well-differentiated and poorly differentiated GCs were cultured in RPMI-1640 medium [FUJIFILM Wako Pure Chemical Corp. (FUJIFILM), Japan] supplemented with 10% FBS (Sigma-Adrich; Merck KGaA), 1% sodium pyruvate (Thermo Fisher Scientific, Inc.), 1% glutamine and 1% penicillin/streptomycin (both from FUJIFILM). 2.0 μg/ml puromycin (Invitrogen; Thermo Fisher Scientific, Inc.) was used for the selection of shRNA-infected cells. All siRNA duplexes were purchased from Gemma (Suzhou, China): non-targeting control siRNA (siCtrl): 5'-UUCUCCGAACGUGUCACGUTT-3' (sense), and siRNA targeting DEK (siDEK): 5'-GUCAGAUGAAUCUAGUAGUTT-3' (sense). The siRNA transfection into AGS cells was performed using Lipofectamine 2000 (Invitrogen; Thermo Fisher Scientific, Inc.) according to the manufacturer's protocol. Cells were harvested after 48 h of siRNA transfection and applied to subsequent RNA-seq. The above-mentioned siRNA sequence and another DEK shRNA were constructed as lentiviral shRNAs: shDEK_1, 5'-GTCAGATGAATCTAGTAGT-3' and shDEK_2, 5'-GAGAGATCAGGTGTAAATAGT-3'. The shRNA-treated cells were harvested after 48 h of puromycin selection for RT-qPCR, immunoblot, and apoptosis assay.

Real-time quantitative polymerase chain reaction (RT-qPCR). An RNeasy Mini Kit (Qiagen GmbH) was used to extract RNA from the GC cell lines. RT-qPCR was performed using the SYBR Green PCR Kit (Toyobo Life Science) on a PicoReal Real-Time PCR system (Thermo Fisher Scientific, Inc.). Glyceraldehyde-3-phosphate dehydrogenase (GAPDH) was used as an internal control. The information in regards to the primers is presented in Table SI. The concentration of each transcript was then normalized to GAPDH mRNA level using the $2^{-\Delta\Delta Cq}$ method (30). We used GraphPad Prism 5 software (GraphPad Software, Inc.) to conduct Student's t-tests.

RNA extraction and high-throughput sequencing. For the RNA-seq, total RNA of the siRNA-treated cells was extracted with Trizol (Ambion; Thermo Fisher Scientific, Inc.) and purified with phenol-chloroform treatments twice. The purified total RNA was treated with RQ1 DNase (RNase-free) (Promega Corp.) to remove the contaminated DNA, and the absorbance at 260/280 nm (A260/A280) was measured using SmartSpec Plus (Bio-Rad Laboratories, Inc.) to determine its quality and quantity. Then, 1.5% agarose gel electrophoresis was used to verify the integrity of the RNA.

For each sample, we used 1.0 μg of total RNA for RNA-seq library preparation by KAPA Stranded mRNA-Seq Kit for Illumina® Platforms (#KK8544; Roche Sequencing and Life Science, USA). Initially, VAHTS mRNA capture beads (N401-01, Vazyme Biotech Co., Ltd.) were used to purify the polyadenylated mRNA. Then, mRNAs were fragmented and converted into double-strand cDNA using KAPA RNA HyperPrep KK8544 (Roche Sequencing and Life Science, USA.). Following end-repair and A tailing, the DNAs were ligated to the Roche Adaptor (KK8726; Roche Sequencing and Life Science, USA.). After purification, these ligated products corresponding to 300-500 bp were amplified, purified, quantified, and stored at -80˚C before sequencing. The strand marked with dUTP (the 2nd cDNA strand) was not amplified, allowing strand-specific sequencing. We used the Illumina Novaseq

6000 system (Illumina, Inc.) to collect data from the 150-nt paired-end sequencing (ABlife Inc.).

RNA-Seq analytical pipeline. First, raw sequencing reads containing more than 2 N-bases were discarded. Then, we used the FASTX-Toolkit (version 0.0.13) (http://hannonlab.cshl.edu/fastx_toolkit) to trim the adaptors and low-quality bases from the raw sequencing reads, and we dropped short reads which were less than 16 nt. After this, the remained sequencing reads were aligned to the GRch38 genome by tophat2 (31) allowing four mismatches. Uniquely mapped reads were used for counting the gene reads, and the FPKM (fragments per kilobase of transcript per million fragments mapped) value was used as an expression level of each gene (32). We obtained all the original sequencing data through our experiment.

Differentially expressed gene (DEG) analysis. We used FPKM to evaluate the gene expression levels, and the R Bioconductor package edgeR (33) was utilized with raw read counts to identify DEGs between the siCtrl and siDEK groups with a critical cut-off at P-value <0.01 and fold changes >1.5 or <2/3.

Alternative splicing analysis. The alternative splicing events (ASEs) and regulated alternative splicing events (RASEs) were defined and quantified by using the ABLas pipeline as described previously (34,35). In brief, ABLas can detect 10 types of ASEs based on splice junction reads, including exon skipping (ES), alternative 5'splice site (A5SS), alternative 3'splice site (A3SS), intron retention (IR), mutually exclusive exons (MXEs), mutually exclusive 5'UTRs (5pMXEs), mutually exclusive 3'UTRs (3pMXEs), cassette exon, A3SS&ES, and A5SS&ES. From the multiple annotated transcripts of each gene, we selected one as the gene model, namely the reference transcript, according to the annotation order, and then analyzed the alternative spliced transcripts relative to the gene model. If one gene splicing site was detected, then multiple transcripts will be detected, and the annotated transcript appearing in the first detection will be used as the model. To assess RASEs, Student's t-test was performed to evaluate the significance of the differences of AS event frequencies between groups. Those events which were significant at a false discovery rate (FDR) cutoff of 5% were considered as RASEs. For the identification of wider ranges of possible ASE candidates, we used simple t-test and P<0.05 was considered as significant.

Functional enrichment analysis. To identify significantly enriched functional categories of DEGs, enrichment of Gene Ontology (GO) terms and Kyoto Encyclopedia of Genes and Genomes (KEGG) pathways were compared between groups using KOBAS 2.0 server (36). In the KOBAS 2.0 platform, transcript length bias (37) was not considered. The enrichment of each pathway (corrected P-value <0.05) was defined using the hypergeometric test and Benjamini-Hochberg FDR correction procedures.

Real time qPCR validation of DEGs and AS events. To elucidate the validity of the RNA-seq data, RT-qPCR was performed for selected DEGs as described above. The PCR conditions consisted of denaturing at 95˚C for 10 min, 40 cycles of denaturing at 95˚C for 15 sec, annealing and extension at 60˚C for 1 min. PCR amplifications were performed in triplicate for each sample. Primers for the qPCR analysis are listed in Table SII.

Immunoblot analysis. Total protein was obtained by RIPA buffer on ice which was separated using 10% SDS-PAGE and blotted onto a PVDF membrane (MilliporeSigma). After blocking using 5% skim milk (FUJIFILM)/0.01% Tween (MP Biomedicals)-TBS, the membranes were incubated with primary antibodies, anti-DEK (1:1,000 dilution; ab166624, Abcam), anti-tubulin (1:2,000 dilution; #62204, Invitrogen; Thermo Fisher Scientific, Inc.) at 4˚C overnight. Then, the membranes were incubated with HRP-conjugated secondary antibodies (anti-mouse IgG; and anti-rabbit IgG, #8460, MBL International Co.) at 1:1,000 dilution for 1 h at room temperature. Signals were developed using Western HRP Substrate (MilliporeSigma) and captured by the ChemiDoc Touch (Bio-Rad Laboratories, Inc.).

Cell apoptosis assay. Cell apoptosis was detected using the Annexin V-FITC Apoptosis Detection Kit (MBL International Co.) according to the manufacturer's protocol. Harvested cells were washed twice with cold PBS and resuspended gently in 85 μl binding buffer, and incubated with 10 μl of Annexin V-FITC and 5 μl propidium iodide (PI) at room temperature for 15 min in the dark. Then, the signals were detected using NovoCyte flow cytometer (ACEA Biosciences).

Statistical analysis. The GraphPad Prism 5 software (GraphPad Software, Inc.) was used to carry out statistical analysis. Each value was acquired from at least three independent experiments. Data are presented as the mean ± SD. A two-tailed unpaired Student's t-test was used to analyze statistical differences between two groups. P<0.05 and <0.01, where appropriate, were considered statistically significant. Where appropriate (Figs. 2A, 3C and D; 4F and G; and 6A-C), one-way ANOVA with Newman-Keuls multiple comparisons test was used to test the statistical significance between multiple groups, and P<0.05 was considered statistically significant.

Results

Expression of DEK is upregulated in GC. In order to confirm that the expression of DEK is upregulated in GC, we used TNMplot web tool (38) to browse available microarray data in the Gene Expression Omnibus (GEO) database (https://www.tnmplot.com/), which included 1,221 and 360 unpaired samples from gastric cancer and normal gastric mucosae, accordingly. The data displayed significantly higher expression in GC tissues in the GEO dataset. Comparison between the normal and tumor samples was performed using Mann-Whitney U test ($P=1.9x10^{-28}$) (Fig. 1A). We also used TNMplot web tool (Bartha and Győrffy, 2021) to browse available RNA-seq data in the The Cancer Genome Atlas (TCGA) database and GTEx database (https://www.tnmplot.com/), which included 375 and 294 unpaired samples from gastric cancer and normal gastric mucosae, accordingly. The data also displayed significantly higher expression in GC tissues. Comparison between the normal and tumor samples was performed using

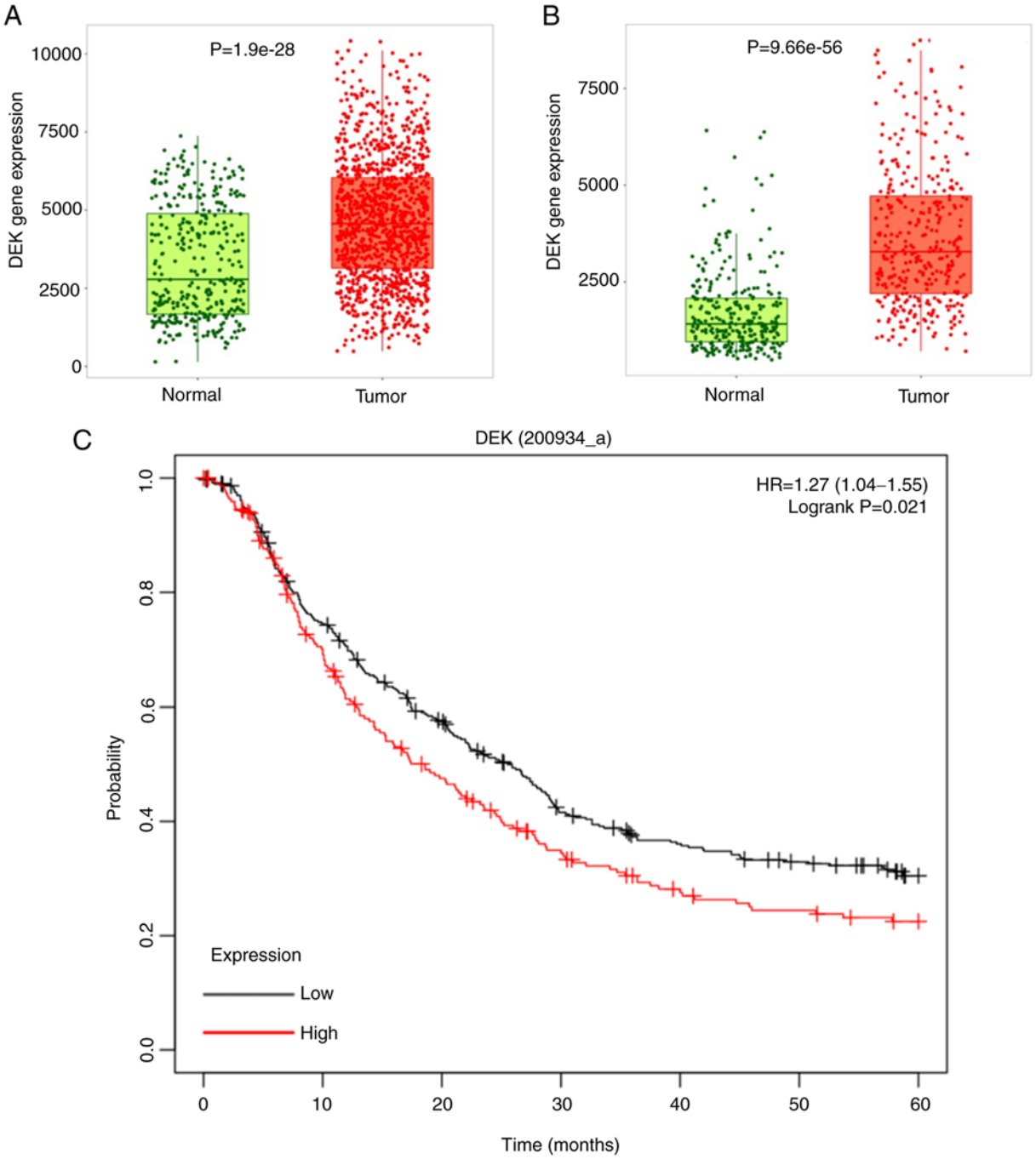

Figure 1. Analysis of DEK expression levels in GC and normal gastric tissues from the GEO, TCGA, and GTEx database. (A) Expression of *DEK* in 360 normal and 1,221 GC samples was plotted as a box-and-whisker plot. The boxplot shows the difference in expression levels between normal and tumor tissues verified by the Wilcox test, and there was a statistically significant difference between the two ($P=1.9x10^{-28}$). In the boxplot, green and red dots represent the corresponding *DEK* gene expression levels of normal samples and tumor samples, respectively. In the box, the upper line of the box represents the upper quartile of *DEK* gene expression, and the lower line represents the lower quartile of *DEK* gene expression. Between the upper line and lower line of the box, the amount of DEK expressed in 50% of the normal and tumor samples is represented. The thick lines in the middle of the green and red boxes indicate the median expression of the *DEK* gene in normal and tumor samples, respectively. (B) The expression of *DEK* in 294 normal and 375 GC samples was plotted as a box-and-whisker plot as in A, and there was a statistically significant difference between the two ($P=9.66x10^{-56}$). Statistical analysis was performed by Student's t-test; P<0.001. (C) Kaplan-Meier curve of GC patients stratified by high or low expression of DEK. Data were obtained from the following datasets. Expression levels of DEK (200934_at) from GSE14210 (N=145), GSE15459 (N=200), GSE22377 (N=43), GSE29272 (N=268), and GSE51105 (N=94). The difference was statistically tested using the log-rank test, P<0.05. GC, gastric cancer; GEO, Gene Expression Omnibus; TCGA, The Cancer Genome Atlas.

Mann-Whitney U test ($P=9.66x10^{-56}$) (Fig. 1B). Moreover, higher expression of DEK was also revealed to be a significant indicator of worse prognosis of GC patients, as revealed by the data from the Kaplan-Meier Plotter (http://kmplot.com/analysis/) (39) (Fig. 1C).

Global gene expression profiles that are regulated by DEK. To investigate DEK-mediated regulation of gene expression, RNA-seq experiments were carried out to compare global gene expression profiles between si*Ctrl*- and si*DEK*-treated human GC cell line AGS. We used two different knockdown

sequences; namely, shDEK_1 and shDEK_2, both of which showed significant knockdown of DEK as shown by RT-qPCR and Immunoblot analysis (Fig. 2A). We used the siRNA containing shDEK_1 sequence for the initial RNA-seq analysis. The cDNA libraries of the siRNA-treated cells (three biological replicates) were constructed which were then sequenced on a next-generation sequencer. Gene expression levels as determined by FPKM values were calculated by an in-house pipeline (see Materials and methods). The effective knockdown of DEK was further confirmed in our RNA-seq analysis (Fig. 2B). FPKM values for all 60,498 gene transcripts were used to calculate a correlation matrix based on Pearson's correlation coefficient (Table SIII), and principal component analysis (PCA) was used to display sample patterns (Fig. 2C). We used logarithmic transformation of expression values for the PCA plot. The PCA showed clearly different distributions between groups; thus, DEK was revealed to affect global and defined gene expression patterns in AGS cells.

Then, we explored gene transcripts whose expression was potentially regulated by DEK. Differentially expressed genes (DEGs) between si*Ctrl*- and si*DEK*-treated AGS cells were identified with cutoff values at fold change (FC) >1.5 or <2/3 to identify upregulated and downregulated genes, respectively. The DEGs related to si*DEK* are displayed in a volcano plot in which genes marked in red and blue represent significantly upregulated and downregulated genes by si*DEK*, respectively (Fig. 2D). A heatmap of the expression patterns of the DEGs showed a high consistency of the siDEK-induced transcription in the biologically triplicated data sets (Fig. 2E). In total, 149 and 229 genes were identified as upregulated and downregulated, respectively, in the *DEK*-knockdown cells (Table SIV). Differentially expressed genes (DEGs) between the si*Ctrl*- and si*DEK*-treated AGS cells were identified with cutoff values at fold change (FC) >3 or <1/3 to identify upregulated and downregulated genes, respectively (Table SV). Differentially expressed genes (DEGs) between si*Ctrl*- and *siDEK*-treated AGS cells were identified with cutoff values at fold change (FC) >4 or <1/4 to identify upregulated and downregulated genes, respectively (Table SVI).

To investigate the potential biological roles of DEK, all the identified DEGs in the *siDEK*-treated AGS cells were subjected to pathway enrichment analyses based on the annotations of GO terms and KEGG pathways. The upregulated and downregulated genes in the si*DEK*-treated cells were enriched in 5 and 6 GO terms, respectively, consisting of 30 and 44 genes including duplicates, respectively (Tables SVII and SVIII). Among the terms of biological processes, the upregulated genes were mainly enriched in 'extracellular matrix organization', 'cell adhesion', 'signal transduction', and 'transmembrane transport' (Fig. 2F). The downregulated genes were largely related to 'nucleosome assembly', 'cellular nitrogen compound metabolism', 'chromatin organization', and 'small molecule metabolism' (Fig. 2G). Among the terms of the KEGG pathways, the upregulated genes were mainly related to 'cytokine-cytokine receptor interaction', 'EMC-receptor interaction', 'hematopoietic cell lineage', and 'chemokine signaling' pathways (Fig. 2H). The downregulated genes were largely related to 'alcoholism', 'systemic lupus erythematosus', 'viral carcinogenesis', and 'transcriptional misregulation in cancer' pathways (Fig. 2I).

DEK globally regulates the expression of multiple cancer-related genes. The 149 upregulated and 229 downregulated genes were identified in the *siDEK* condition (Table SIV). Among them, RNA-seq data of a representatively selected 7 upregulated genes, *ACTA2*, *CXCL10*, *HMOX1*, *SPRR2A*, *KIFC3*, *OSBPL5*, and *CCDC80*, and 9 downregulated genes, *ASNS*, *CHAC1*, *DDIT4*, *ERRFI1*, *FAM3C*, *JDP2*, *PSAT1*, *PSPH*, and *RMRP* are shown in Fig. 3A and B. These genes were significantly upregulated or downregulated in the *siDEK* condition as well as identified in the categories of significantly enriched GO biological processes in our analysis and have also been known to be linked to cancer development with respect to apoptosis, invasion, proliferation, or migration of cancer cells (40-55). In order to verify the RNA-seq results, we conducted RT-qPCR analysis. The shRNAs containing scramble control, shDEK_1, and shDEK_2 were infected into AGS and NUGC4 cells. A representative upregulated DEG and two representative downregulated DEGs, including *CCDC80*, *PSAT1*, and *PSPH*, were subjected to RT-qPCR analysis. The results of this experiment are presented in Fig. 3C and D. RNA-seq results were confirmed in all the candidate genes investigated in both AGS and NUGC4 cells treated with two different shRNA sequences (Fig. 3C and D). Based on public datasets of gene expression profiles of GC cases, it was revealed that some, if not all, of the representative upregulated and downregulated genes identified in this study, were negatively and positively correlated with DEK expression, respectively, in clinical GC samples (Fig. 3E). Furthermore, these representative genes were also significantly associated with better and worse prognoses of GC patients, respectively, in some, if not all, of the independent public datasets (Fig. 3F). These results conclude that DEK globally regulates the expression of multiple oncogenes and tumor-suppressor genes. These statistical correlations were only modest and more precise investigation with larger cohorts will be necessary in future research.

DEK globally regulates alternative splicing of multiple cancer-related genes. To gain further insights into the role of DEK on alternative splicing regulation, we analyzed RNA-seq data to explore the DEK-mediated alternative splicing events (ASEs) in the human GC cell line AGS. We detected 62.48% (229,508 out of 367,321) of the annotated exons, confirmed a total of 149,370 known splicing sites, and found 132,858 novel splicing sites (Tables SIX and X). We then analyzed the ASEs and detected a total of 16,536 known ASEs in reference genes and 42,229 novel ASEs, excluding intron retention (IR) (Table SXI).

In order to further analyze the differences in frequencies of the alternative splicing that were probably regulated by DEK [named regulated ASEs (RASEs)], we statistically compared the ASE profiles of siCtrl and siDEK conditions using a t-test with a criterion of P-value ≤0.05. RASEs with t-values >0 and <0 were marked as AS-up and -down, respectively. In total, we identified 1,036 RASEs (Table SXII), which consisted of 218 IR RASEs (including 51 known RASEs) and 818 non-IR (NIR) RASEs.

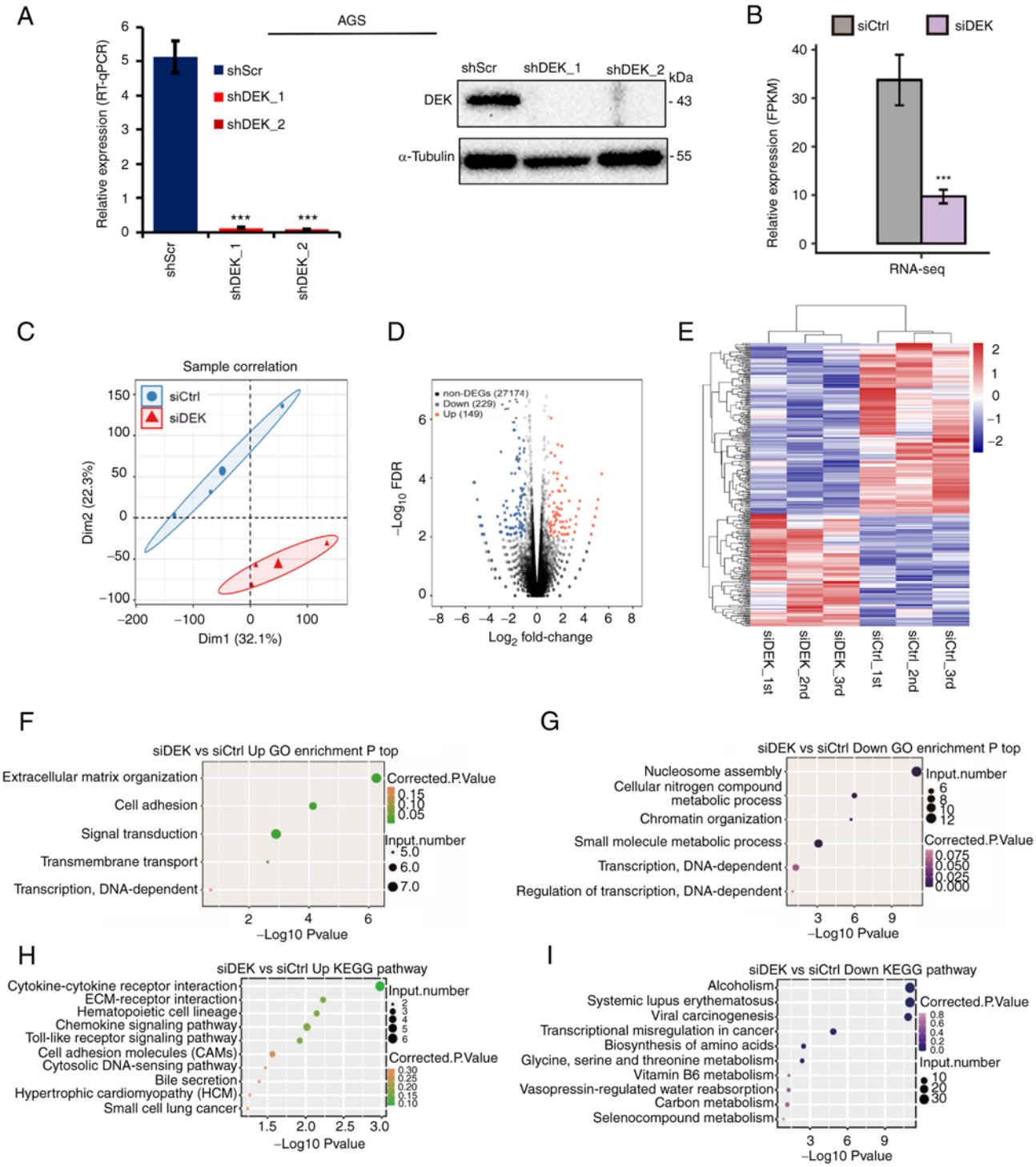

Figure 2. Global picture of the DEK-regulated transcriptome in a human GC cell line AGS. (A) Relative mRNA expression levels of *DEK* (% of GAPDH) in shRNA-infected cells as assessed by RT-qPCR are shown in the left panel. Statistical differences between groups (shScr and either shDEK_1 or shDEK_2) were tested using one-way ANOVA with Newman-Keuls multiple comparisons test, and P<0.05 was considered statistically significant. Bars and error bars represent the mean ± SD, respectively (n=3), ***P<0.001. Protein levels of DEK and α-tubulin in shRNA-infected cells as assessed by immunoblots are shown with their molecular sizes (kDa) in the right panel. (B) DEK expression (FPKM value) was quantified by RNA-seq. Error bars represent mean ± SEM, ***P<0.001. (C) Principal component analysis of the six samples consisting of the biological triplicates of si*Ctrl*- and si*DEK*-treated cells based on the normalized gene expression levels. The abscissa represents dimension 1, the ordinate represents dimension 2; the three small dots in the blue ellipse represent the three samples of the si*Ctrl* group, and the large dot in the middle is the normalization of the si*Ctrl* group again. The three small triangles in the red ellipse represent the three samples of the si*DEK* group, and the large triangle in the middle is the normalization of the si*DEK* group again. (D) A volcano plot for the identification of DEK-regulated genes. Significantly upregulated and downregulated genes are labeled in red and blue, respectively. (E) Hierarchical clustering of the DEGs in the si*Ctrl*- and si*DEK*-treated AGC cells. FPKM values are log2-transformed and then median-centered by each gene. Expression values are indicated as gradient blue-to-red colors as indicated at the right side of the figure. (F and G) The five and six GO biological processes of the upregulated and downregulated genes, respectively. Corrected P-values and annotated gene numbers in each category are indicated as colors and sizes of the dots, respectively, as indicated at the right sides of each figure. (H and I) The top 10 representatives KEGG pathway of the upregulated and downregulated genes, respectively. Corrected P-values and annotated gene numbers in each category are indicated as colors and sizes of the dots, respectively, as indicated at the right sides of each figure. GC, gastric cancer; FPKM, fragments per kilobase of transcript per million fragments mapped; DEGs, differentially expressed genes; GO, Gene Ontology; KEGG, Kyoto Encyclopedia of Genes and Genomes.

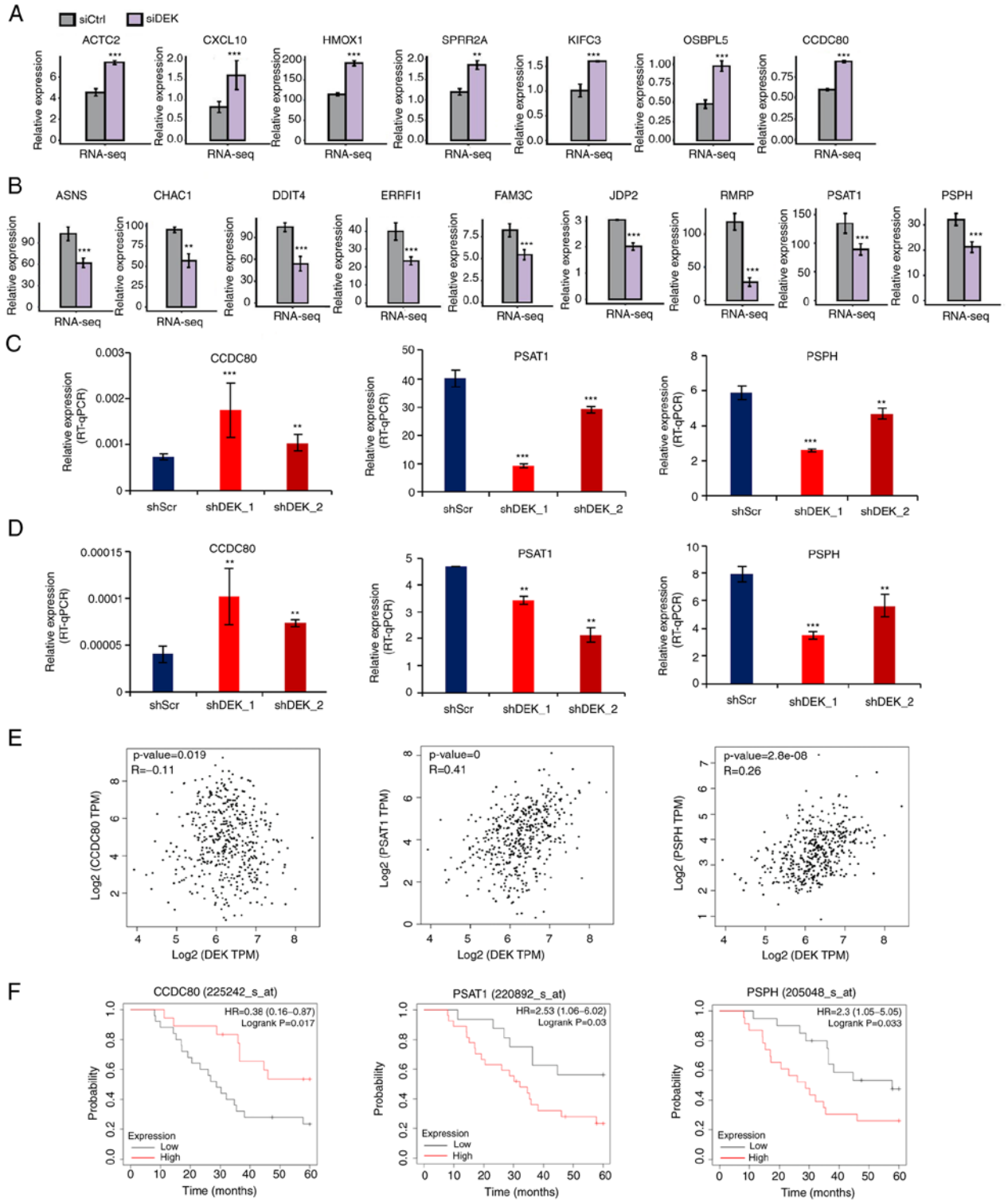

Figure 3. Representative genes whose expression is potentially regulated by DEK. (A and B) FPKM values of representative DEGs that were significantly upregulated or downregulated in the si*DEK* condition in a human GC cell line AGS are shown as bar plots. Gray and purple bars show the FPKM values of the si*Ctrl*- and si*DEK*-treated AGS cells, respectively. Bars and error bars represent means and SEMs, respectively. **P<0.01, ***P<0.001. (C and D) Relative expression levels of DEGs (% of GAPDH) in shRNA-infected cells in AGS and NUGC4 cell lines were validated by RT-qPCR assay, respectively. Statistical differences between groups (shScr and either shDEK_1 or shDEK_2) were tested using one-way ANOVA with Newman-Keuls multiple comparisons test, and P<0.05 was considered statistically significant. Bars and error bars represent the mean ± SD, respectively (n=3). **P<0.01, ***P<0.001. (E) Correlation of gene expression levels between *DEK* and *CCDC80*, *PSAT1* and *PSPH* from public datasets are shown as dot plots. Each dot represents a single GC case. All the data were derived from the GEPIA2 database (http://gepia2.cancer-pku.cn/#correlation). (F) Kaplan-Meier curves of GC patients as stratified with high and low expression levels of CCDC80, PSAT1 and PSPH. All of the data were obtained from the GSE22377 (N=43) dataset. (http://kmplot.com/analysis/index.php?p=service&cancer=gastric). P-values were calculated by log-rank test. GC, gastric cancer; FPKM, fragments per kilobase of transcript per million fragments mapped; DEGs, differentially expressed genes; ACTA2, alpha smooth muscle actin; CXCL10, chemokine (C-X-C motif) ligand 10; HMOX1, heme oxygenase-1; SPRR2A, small proline-rich protein 2A; KIFC3, kinesin family member C3; OSBPL5, oxysterol binding protein like 5; CCDC80, coiled-coil domain containing 80; ASNS, asparagine synthetase; CHAC1, cation transport regulator 1; DDIT4, DNA damage-inducible transcript 4; ERRFI1, ERBB receptor feedback inhibitor 1; FAM3C, FAM3 metabolism regulating signaling molecule C; JDP2, Jun dimerization protein 2; RMRP, RNA component of mitochondrial RNA processing; PSAT1, phosphoserine aminotransferase 1; PSPH, phosphoserine phosphatase.

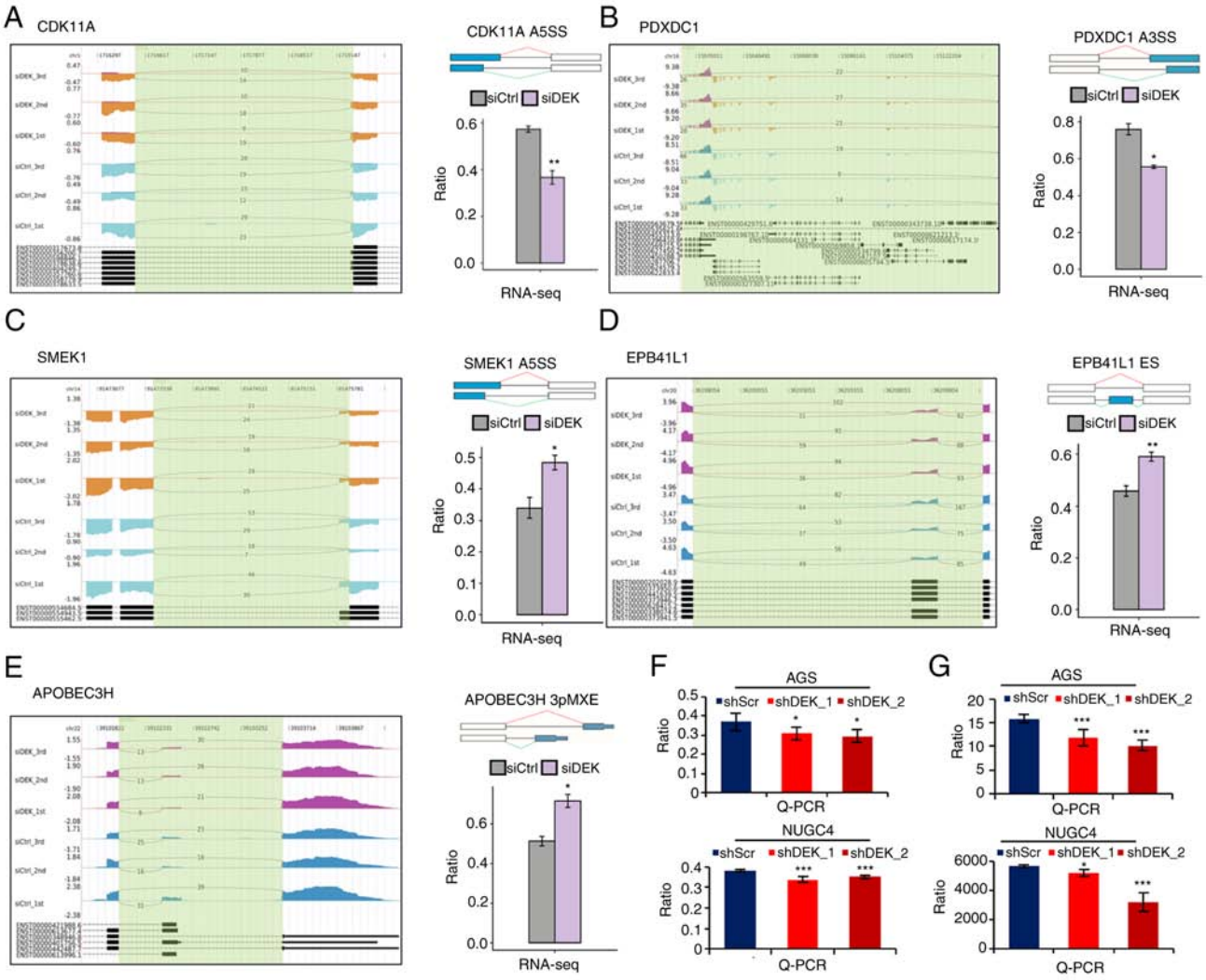

Figure 4. DEK-regulated ASEs of the different gene transcripts. (A-E) IGV-sashimi plots show the AS changes in the si*DEK* conditions compared to the si*Ctrl*. The y-axis represents the corresponding sequence reads; the larger the area, the more abundant the corresponding transcript is. Read distributions were mapped either from 5'→3' (positive values) or from 3'→5' (negative values) according to the corresponding sequences of the human genome. The bottom of each figure exhibits the annotated exons of the gene. The schematic diagram at the right upper panel of each figure depicts the structure of ASE, AS1 (shown in green) and AS2 (shown in red). The exons and introns are denoted as boxes and lines, respectively, while the alternatively spliced exons are shown as blue boxes. RNA-seq quantification of the ASEs is shown as a bar graph. The y-axis represents the altered ratio of ASEs calculated by the following formula: (alternative splice junction reads/total sequence reads of the splice junction). Student's t-test was performed to compare the values between the si*DEK* and si*Ctrl* conditions. *P<0.05, **P<0.01. (F and G) RT-qPCR validation of representative DEK-regulated alternative splicing events in CDK11A and PDXDC1 transcripts shown in A and B. Validating RT-qPCRs were performed in AGS and NUGC4 cell lines. The y-axis represents the altered ratio of ASEs calculated by the following formula: (AS1 transcripts level/AS2 transcripts level). Statistical differences between groups (shScr and either shDEK_1 or shDEK_2) were tested using one-way ANOVA with Newman-Keuls multiple comparisons test, and P<0.05 was considered statistically significant. Bars and error bars represent the mean ± SD, respectively (n=3). *P<0.05, ***P<0.001. ASEs, alternative splicing events; CDK11A, cyclin-dependent kinase 11A; PDXDC1, pyridoxal-dependent decarboxylase domain-containing 1; SMEK1, SMEK homolog 1; EPB41L1, erythrocyte membrane protein band 4.1 like 1; APOBEC3H, apolipoprotein B mRNA editing enzyme catalytic subunit 3H.

ASEs are mainly classified into various subtypes such as alternative 5'splice site (A5SS), mutually exclusive exon (MXE), mutually exclusive 5'UTR (5PMXE), exon skipping (ES), alternative 3'splice site (A3SS), intron resist (IntronR), mutually exclusive 3'UTRS (3PMXE), A3SS&ES, cassette exon, and A5SS&ES (56). Representative schemas of the ASEs in *CDK11A* (A5SS), *SMEK1* (A5SS), *EPB41L1* (ES), *PDXDC1* (A3SS), and *APOBEC3H* (3PMXE) transcripts are displayed in Fig. 4A-E, where significant differences in the frequency of ASEs between *siDEK* and *siCtrl* conditions are shown. These representative genes have been reported to be associated with multiple molecular mechanisms related to carcinogenesis (57-61). To validate DEK-regulated alternative splicing events identified from the RNA-seq data in this study, we performed RT-qPCR to quantify the frequencies of candidate splicing events, using two different cell lines, AGS and NUGC4, treated with two independent shRNA sequences, shDEK_1 and shDEK_2 (Fig. 4F and G). PCR primer pairs are listed in Table SII, which were designed to specifically amplify either longer or shorter splicing isoforms. Candidate alternative splicing events in *CDK11A* and *PDXDC1* genes were clearly validated by RT-qPCR in agreement with the RNA-seq results (Fig. 4F and G). Due to the technical difficulties such as in designing primers which specifically amplify designated splicing isoforms, further validation of other splicing events

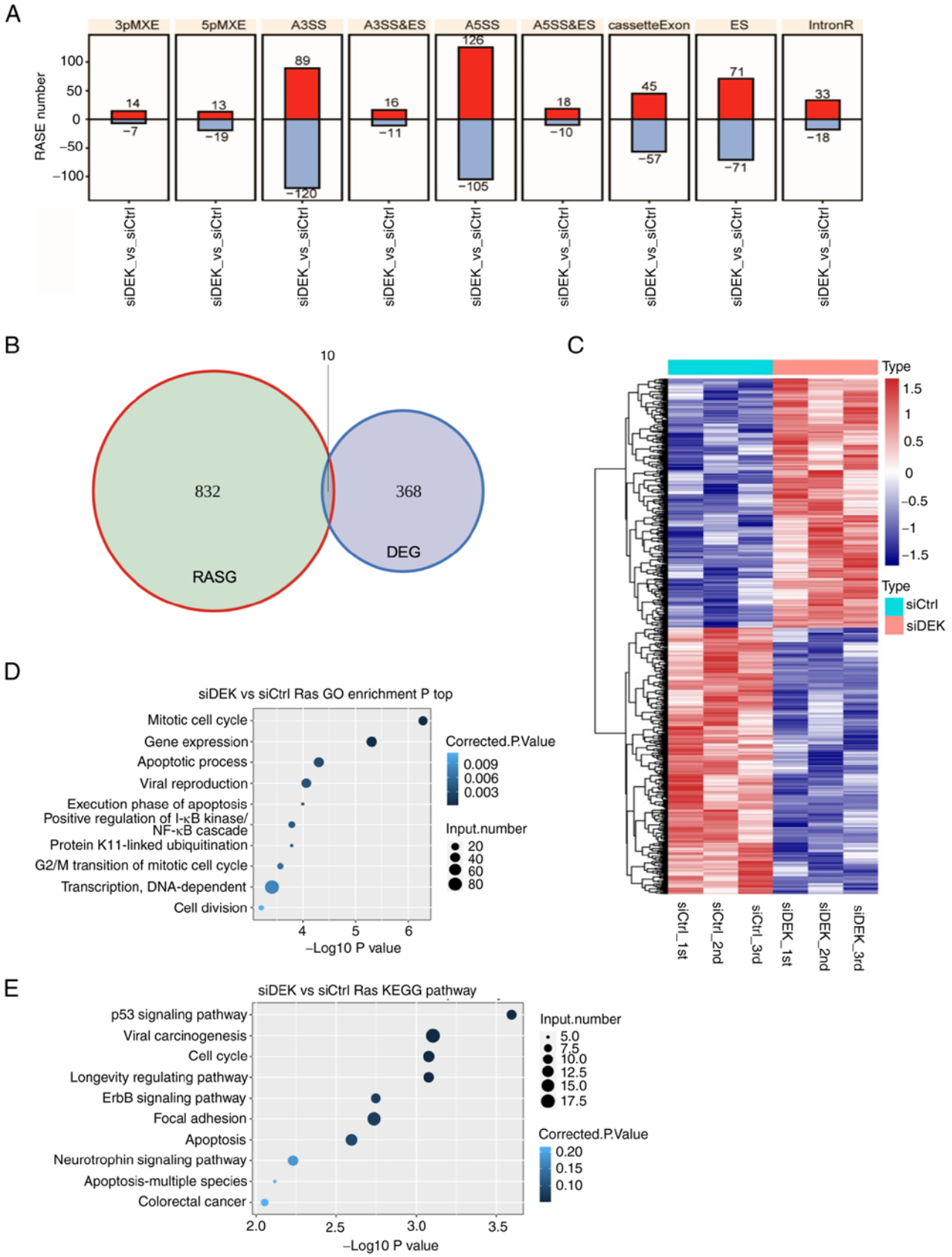

Figure 5. Global picture of the RASEs that are regulated by DEK. (A) Frequency distributions of different types of DEK-regulated ASEs. Red and blue bars represent the increase and decrease in the numbers of RASEs in the si*DEK* condition, respectively. The y-axis represents the number of genes. (B) The overlap between DEGs and DEK-regulated ASEs is shown as a Venn diagram. Numbers represent gene numbers in each category. (C) Hierarchical clustering of the frequencies of ASEs in genes in the si*Ctrl* and si*DEK* conditions. Frequencies of the ASEs are shown as gradient colors of blue and red, as indicated at the right side of the figure. (D and E) The top 10 most enriched pathways of GO biological processes and KEGG pathways among the RASGs. The corrected P-values and number of genes in each category are indicated as colors and sizes of dots, as indicated at the right sides of the figures. RASEs, regulated alternative splicing events; DEGs, differentially expressed genes; RASGs, regulated alternative splicing genes; GO, Gene Ontology; KEGG, Kyoto Encyclopedia of Genes and Genomes; A3SS&ES, alternative 3'splice site and exon skipping; A5SS&ES, alternative 5'splice site and exon skipping MXEs mutually exclusive exon.

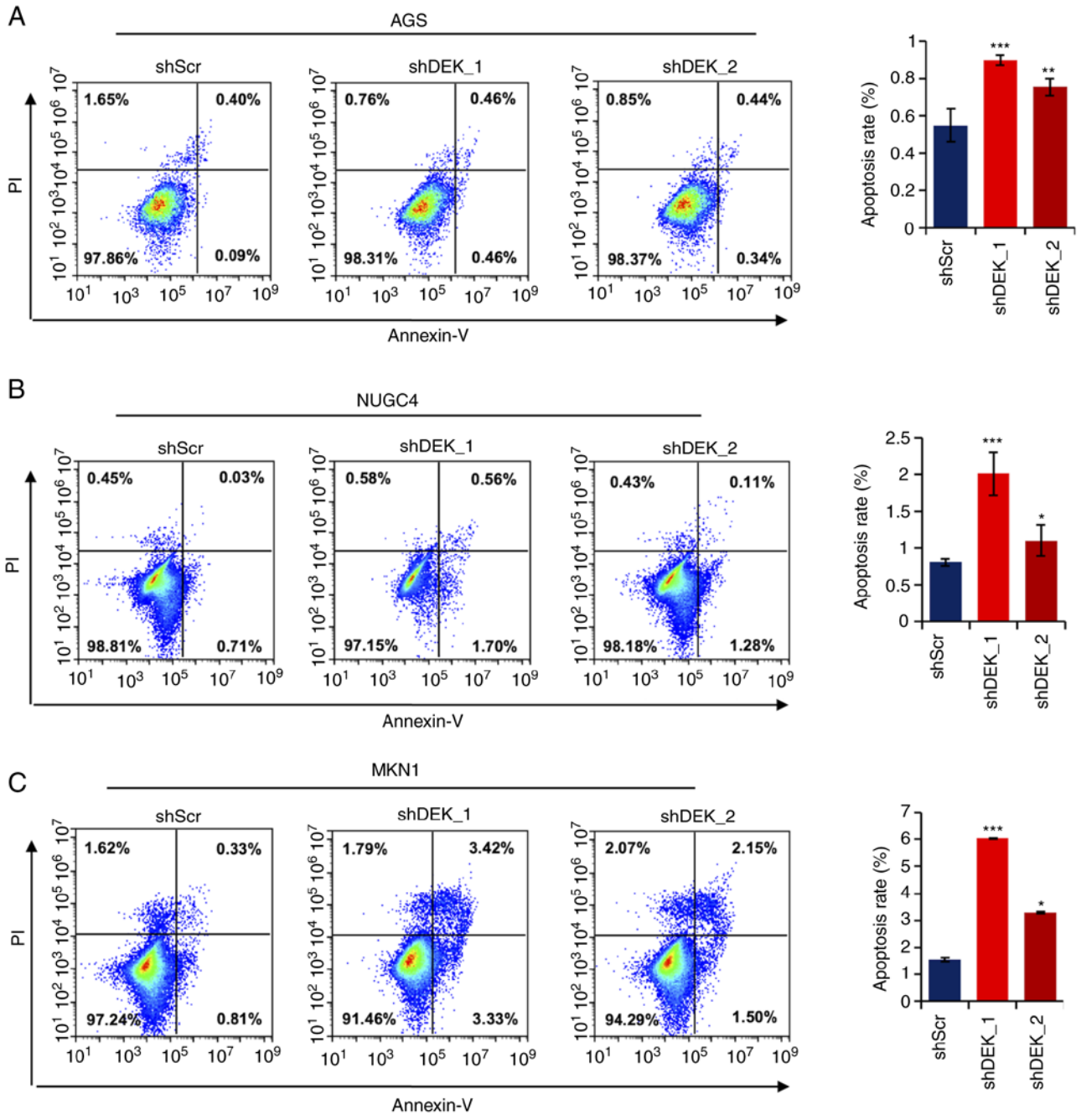

Figure 6. DEK knockdown induces apoptosis in GC cells. (A-C) Frequencies of apoptotic cells were assessed by flow cytometry in three different GC cell lines. The x- and y-axis represent the signal intensities of Annexin V and PI, respectively. Quantitative data are shown at the right side. Statistical differences between groups (shScr and either shDEK_1 or shDEK_2) were tested using one-way ANOVA with Newman-Keuls multiple comparisons test, and P<0.05 was considered statistically significant. Bars and error bars represent the mean ± SD, respectively (n=3). *P<0.05, **P<0.01, ***P<0.001. GC, gastric cancer.

identified in the RNA-seq remains to be conducted in the next research plan.

Among the various subtypes of ASEs, the majority of the RASEs identified in this study were A5SS (231 events), A3SS (209 events), and ES (142 events) (Fig. 5A). These data clearly indicated that DEK globally regulates ASEs in the human GC cell line AGS. To investigate whether or not DEK simultaneously regulates gene expression and alternative splicing on the same set of target genes, we explored the overlaps of the RASEs and DEGs identified in our analyses. It was revealed that only 10 genes commonly exhibited significant differences in both expression levels and splicing events (Fig. 5B and Table SXIII), suggesting that DEK regulates gene expression and alternative splicing in different mechanisms. A heat map analysis of the frequencies of RASEs in affected genes clearly showed substantially high consistencies of the siDEK-induced ASEs in the biologically triplicated cells (Fig. 5C). Pathway enrichment analyses were further conducted to identify possible biological impacts of these DEK-mediated RASGs (regulated alternative splicing genes) in a global manner, revealing that the RASGs in the siDEK condition were highly enriched for genes related to 'mitotic cell cycle', 'gene expression', and 'apoptotic process' pathways among others based on the GO biological process terms (Fig. 5D and Table SXIV). In regards to the KEGG

pathways, RASEs were likely enriched in 'p53 signaling', although statistically not significant (Fig. 5E and Table SXV).

The whole genomic profiling of the RASGs by the RNA-seq of a human GC cell line AGS with or without DEK knockdown revealed that DEK globally regulates not only gene expression but also alternative splicing in multiple important cancer-related genes and pathways. Thus, DEK possibly plays important role in gastric tumorigenesis.

DEK knockdown induces apoptosis in gastric cancer cells. To examine whether DEK knockdown affects apoptotic pathways as revealed by the GO analysis above, we examined frequencies of apoptosis in cells treated with shRNAs for DEK. As shown in Fig. 6A, in all the gastric cancer cell lines investigated, AGS, NUGC4, and MKN1, the frequencies of apoptotic cells were significantly increased in both the shDEK_1-treated and shDEK_2-treated cells (Fig. 6A-C). These data robustly reveal that *DEK* knockdown significantly induces apoptosis in GC cells.

Discussion

The present study, for the first time, clarified whole-genomic images of DEK-mediated gene regulations both from transcription and alternative splicing levels in a human GC cell line. Although DEK has been thought to play oncogenic roles in various malignancies (6,7,27,62-64), its precise mechanisms of gene regulation remain elusive. This study confirmed previous knowledge that DEK is overexpressed in GC as well as is a prognostic marker for GC patients; moreover, our results showed that DEK simultaneously affects a number of genes in important cancer-related pathways, supporting its oncogenic roles in gastric carcinogenesis.

Focusing on important cancer-related genes which we found are positively regulated by DEK, expression of phosphoserine aminotransferase 1 (*PSAT1*) and phosphoserine phosphatase (*PSPH*), for instance, also showed mild but significant positive correlations with DEK expression among GC samples in public datasets; moreover, higher expression of those genes indicated significantly worse prognoses of GC patients. These observations are consistent with the molecular functions of these genes. In that, PSAT1 overexpression has been observed in multiple tumor types and is associated with poorer clinical outcomes, related to EGFR activation (65), and PSAT1 contributes to lung cancer cell migration in part by promoting nuclear PKM2 translocation (65). PSPH promotes melanoma growth and metastasis by metabolic deregulation-mediated transcriptional activation of NR4A1 (54). On the other hand, among genes that we discovered to be negatively regulated by DEK, negative correlations of expression with DEK and prognostic significance of coiled-coil domain containing 80 (*CCDC80*) were confirmed in public datasets of GC cases. *CCDC80* is known to be a pro-apoptotic molecule and its expression is positively correlated with that of E-cadherin in thyroid carcinoma and is also identified as a strong suppressor for colitis and colorectal carcinogenesis (40,66). Therefore, it can be concluded that DEK regulates the expression levels of important oncogenes and tumor-suppressor genes.

However, since DEK simultaneously regulates a substantially wide variety of target genes at a time, functional inconsistencies were also identified; such that DEK could positively and negatively regulate the expression of tumor suppressors and oncogenes, respectively. For example, and not limited to, *KIFC3* and *OSBPL5* which were negatively regulated by DEK, where *siDEK* upregulated their expression, are well-known oncogenes (44,46,67). DEK has been reported to inhibit cell differentiation, senescence, and apoptosis, and to promote cell survival and proliferation in cancer cells (22). Based on the finding in this study, it is considered that these oncogenic phenotypes exerted by DEK are the consequences of the combinations of the global gene regulatory network of DEK that can work providing both oncogenic and tumor-suppressive potential. Further investigations focusing on not only molecular functions of each target gene but also the context-dependent interactions of DEK-mediated global modifications of signaling pathways will be required to fully clarify the oncogenic function of DEK.

Our study is the first one where DEK-mediated alternative splicing events were investigated in a whole-genomic manner, revealing that DEK affected substantially large numbers of alternative splicing in a GC cell line. In the present study, it was revealed that at least 832 transcripts were significantly regulated by DEK in a GC cell line. Many of the DEK-mediated alternative splicing events (ASEs) were identified as A5SS and A3SS, which is consistent with the function of DEK in which DEK enforces discriminations by U2AF between 3'splicing cites AG and CG (13). Importantly, we found that many ASEs were found in transcripts of important oncogenes and tumor-suppressor genes, including *CDK11A*, *SMEK1*, *EPB41L1*, *PDXDC1*, and *APOBEC3H*. SMEK homolog 1 (*SMEK1*) was reported to exert its antitumor role by inhibiting the phosphorylation of Akt/mTOR in ovarian cancers (58). Erythrocyte membrane protein band 4.1 like 1 (*EPB41L1*) plays a tumor-suppressive role by affecting Wnt/β-catenin signaling in non-small cell lung cancers (59). On the other hand, among such RASEs of DEK, cyclin-dependent kinase 11A (*CDK11A*) is a well-known oncogene (57). Pyridoxal-dependent decarboxylase domain-containing 1 (*PDXDC1*) is reported to be somatically mutated in renal cell cancers (60), although its cancer-related function has not been established. Apolipoprotein B mRNA editing enzyme catalytic subunit 3H (*APOBEC3H*) is known to regulate the integrity of the genome (61). Importantly, functional consequences of the alternative splicing in genes are biologically difficult to predict. If the alternative splice site events (e.g., A5SS and A3SS which we found frequently in our dataset) result in frameshifts of the affected transcripts, it would be considered to result in loss-of-function of the gene. However, if alternative splicing created in-frame variants of genes, their molecular functions are not easily assumed and require extensive biological investigations of the affected transcript. Thus, although we could identify a global catalog of ASEs that were regulated by DEK, their molecular consequences should be investigated further to fully clarify the molecular functions of affected genes as well as the context-dependent regulatory networks of those DEK-mediated ASEs in view of global signaling pathways in cancer cells.

The sequence organization and DNA-binding and RNA-binding properties of DEK suggest that it could have dual functions in the mRNA synthesis at the transcriptional and post-transcriptional levels. An intriguing question is whether or not DEK regulates both gene expression and alternative splicing on the overlapped targets. In the present study, it was revealed that the overlaps between the DEK-mediated regulations of gene expression and those of ASEs are almost negligible, indicating that the molecular mechanisms of DEK-mediated transcription regulation and post-transcriptional splicing modification should be exerted in different types of machinery. It would be a scientifically important issue to identify various subsets of protein-protein complexes of DEK-related machinery and reveal their molecular function in either transcriptional and post-transcriptional regulations.

In the present study, we successfully applied RNA-seq technology to investigate the role of DEK in a human GC cell line, demonstrating that DEK regulates both transcription and alternative splicing in a number of genes some of which are significantly enriched in important cancer-related pathways. DEK has been reported to play pivotal oncogenic roles in various malignancies, and our study at least in part shed light on its molecular mechanisms. Further molecular investigations of the target genes of DEK that our RNA-seq pointed out would further help develop DEK as a diagnostic and therapeutic target for GC.

Acknowledgements

We are very grateful to Dr Shumpei Ishikawa and Dr Hiroto Katoh for their thoughtful discussion of this study.

Funding

This research was partly supported by grants from the China Scholarship Council (no. 202006170206) to B.L. This research was supported by the Natural Science Foundation of Jilin Province, China (no. 20200201168JC) to J.S.

Availability of data and materials

The datasets analyzed during the current study are available in SRA (https://www.ncbi.nlm.nih.gov/sra, PRJNA743794).

Authors' contributions

BL performed the experiments, contributed to analysis and interpretation of the data, and was a major contributor in writing the manuscript. YS and JS performed the experiments, and contributed to the drafting and revision of the manuscript. YZ, JS and YX contributed to the conception and design of the study, the data analysis and interpretation, and the writing and revision of the manuscript. All authors read and approved the manuscript and agree to be accountable for all aspects of the research in ensuring that the accuracy or integrity of any part of the work (in particular the provided data) are appropriately investigated and resolved.

Ethics approval and consent to participate

Not applicable.

Patient consent for publication

Not applicable.

Competing interests

The authors declare that they have no competing interests.

References

1. Khan SA, Amnekar R, Khade B, Barreto SG, Ramadwar M, Shrikhande SV and Gupta S: p38-MAPK/MSK1-mediated overexpression of histone H3 serine 10 phosphorylation defines distance-dependent prognostic value of negative resection margin in gastric cancer. Clin Epigenetics 8: 88, 2016.
2. Matsusaka K, Ushiku T, Urabe M, Fukuyo M, Abe H, Ishikawa S, Seto Y, Aburatani H, Hamakubo T, Kaneda A and Fukayama M: Coupling CDH17 and CLDN18 markers for comprehensive membrane-targeted detection of human gastric cancer. Oncotarget 7: 64168-64181, 2016.
3. Wang YY, Jiang WL, Zhang PF, Li GF, Dong JH and Wang XS: Oct-4 is associated with gastric cancer progression and prognosis. OncoTargets Ther 9: 517-522, 2016.
4. Ford AC, Yuan Y and Moayyedi P: *Helicobacter pylori* eradication therapy to prevent gastric cancer: Systematic review and meta-analysis. Gut 69: 2113-2121, 2020.
5. Yang X, Takano Y and Zheng HC: The pathobiological features of gastrointestinal cancers (Review). Oncol Lett 3: 961-969, 2012.
6. von Lindern M, Fornerod M, van Baal S, Jaegle M, de Wit T, Buijs A and Grosveld G: The translocation (6;9), associated with a specific subtype of acute myeloid leukemia, results in the fusion of two genes, dek and can, and the expression of a chimeric, leukemia-specific dek-can mRNA. Mol Cell Biol 12: 1687-1697, 1992.
7. Wise-Draper TM, Allen HV, Jones EE, Habash KB, Matsuo H and Wells SI: Apoptosis inhibition by the human DEK oncoprotein involves interference with p53 functions. Mol Cell Biol 26: 7506-7519, 2006.
8. Carro MS, Spiga FM, Quarto M, Ninni VD, Volorio S, Alcalay M and Müller H: DEK expression is controlled by E2F and deregulated in diverse tumor type. Cell Cycle 5: 1202-1207, 2006.
9. Liu G, Xiong D, Zeng J, Xu G, Xiao R, Chen B and Huang Z: Prognostic role of DEK in human solid tumors: A meta-analysis. Oncotarget 8: 98985-98992, 2017.
10. Kappes F, Waldmann T, Mathew V, Yu J, Zhang L, Khodadoust MS, Chinnaiyan AM, Luger K, Erhardt S, Schneider R and Markovitz DM: The DEK oncoprotein is a Su(var) that is essential to heterochromatin integrity. Genes Dev 25: 673-678, 2011.
11. Fu GK, Grosveld G and Markovitz DM: DEK, an autoantigen involved in a chromosomal translocation in acute myelogenous leukemia, binds to the HIV-2 enhancer. Proc Natl Acad Sci 94: 1811-1815, 1997.
12. McGarvey T, Rosonina E, McCracken S, Li Q, Arnaout R, Mientjes E, Nickerson JA, Awrey D, Greenblatt J, Grosveld G and Blencowe BJ: The acute myeloid leukemia-associated protein, DEK, forms a splicing-dependent interaction with exon-product complexes. J Cell Biol 150: 309-320, 2000.
13. Soares LMM, Zanier K, Mackereth C, Sattler M and Valcárcel J: Intron removal requires proofreading of U2AF/3'splice site recognition by DEK. Science 312: 1961-1965, 2006.
14. Waldmann T: Structure-specific binding of the proto-oncogene protein DEK to DNA. Nucleic Acids Res 31: 7003-7010, 2003.
15. Alexiadis V, Waldmann T, Andersen J, Mann M, Knippers R and Gruss C: The protein encoded by the proto-oncogene DEK changes the topology of chromatin and reduces the efficiency of DNA replication in a chromatin-specific manner. Genes Dev 14: 1308-1312, 2000.
16. Kavanaugh GM, Wise-Draper TM, Morreale RJ, Morrison MA, Gole B, Schwemberger S, Tichy ED, Lu L, Babcock GF, Wells JM, *et al*: The human DEK oncogene regulates DNA damage response signaling and repair. Nucleic Acids Res 39: 7465-7476, 2011.
17. Waldmann T, Scholten I, Kappes F, Hu HG and Knippers R: The DEK protein-an abundant and ubiquitous constituent of mammalian chromatin. Gene 343: 1-9, 2004.

18. Modrek B and Lee C: A genomic view of alternative splicing. Nat Genet 30: 13-19, 2002.
19. Pan Q, Shai O, Lee LJ, Frey BJ and Blencowe BJ: Deep surveying of alternative splicing complexity in the human transcriptome by high-throughput sequencing. Nat Genet 40: 1413-1415, 2008.
20. Chen J and Weiss WA: Alternative splicing in cancer: Implications for biology and therapy. Oncogene 34: 1-14, 2015.
21. Kress TL and Guthrie C: Accurate RNA siting and splicing gets help from a DEK-Hand. Science 312: 1886-1887, 2006.
22. Wise-Draper TM, Mintz-Cole RA, Morris TA, Simpson DS, Wikenheiser-Brokamp KA, Currier MA, Cripe TP, Grosveld GC and Wells SI: Overexpression of the Cellular DEK protein promotes epithelial transformation in vitro and in vivo. Cancer Res 69: 1792-1799, 2009.
23. Pease NA, Wise-Draper T and Privette Vinnedge L: Dissecting the potential interplay of DEK functions in inflammation and cancer. J Oncol 2015: 106517, 2015.
24. Piao J, Shang Y, Liu S, Piao Y, Cui X, Li Y and Lin Z: High expression of DEK predicts poor prognosis of gastric adenocarcinoma. Diagn Pathol 9: 67, 2014.
25. Ou Y, Xia R, Kong F, Zhang X, Yu S, Jiang L and Zheng L: Overexpression of DEK is an indicator of poor prognosis in patients with gastric adenocarcinoma. Oncol Lett 11: 1823-1828, 2016.
26. Lin KH and Tsai CY: Overexpression of DEK in human gastric carcinoma and its clinicopathological significance. J Clin Oncol 33: 75-75, 2015.
27. Wang J, Wen T, Li Z, Che X, Gong L, Jiao Z, Qu X and Liu Y: CD36 upregulates DEK transcription and promotes cell migration and invasion via GSK-3β/β-catenin-mediated epithelial-to-mesenchymal transition in gastric cancer. Aging (Albany NY) 13: 1883-1897, 2020.
28. Hui W, Ma X, Zan Y, Song L, Zhang S and Dong L: MicroRNA-1292-5p inhibits cell growth, migration and invasion of gastric carcinoma by targeting DEK. Am J Cancer Res 8: 1228-1238, 2018.
29. Zhang W, Liao K and Liu D: MiR-138-5p inhibits the proliferation of gastric cancer cells by targeting DEK. Cancer Manag Res 12: 8137-8147, 2020.
30. Livak KJ and Schmittgen TD: Analysis of relative gene expression data using real-time quantitative PCR and the 2(-Delta Delta C(T)) method. Methods 25: 402-408, 2001.
31. Kim D, Pertea G, Trapnell C, Pimentel H, Kelley R and Salzberg SL: TopHat2: Accurate alignment of transcriptomes in the presence of insertions, deletions and gene fusions. Genome Biol 14: R36, 2013.
32. Trapnell C, Williams BA, Pertea G, Mortazavi A, Kwan G, van Baren MJ, Salzberg SL, Wold BJ and Pachter L: Transcript assembly and quantification by RNA-Seq reveals unannotated transcripts and isoform switching during cell differentiation. Nat Biotechnol 28: 511-515, 2010.
33. Robinson MD, McCarthy DJ and Smyth GK: edgeR: A Bioconductor package for differential expression analysis of digital gene expression data. Bioinformatics 26: 139-140, 2010.
34. Jin L, Li G, Yu D, Huang W, Cheng C, Liao S, Wu Q and Zhang Y: Transcriptome analysis reveals the complexity of alternative splicing regulation in the fungus Verticillium dahliae. BMC Genomics 18: 130, 2017.
35. Xia H, Chen D, Wu Q, Wu G, Zhou Y, Zhang Y and Zhang L: CELF1 preferentially binds to exon-intron boundary and regulates alternative splicing in HeLa cells. Biochim Biophys Acta Gene Regul Mech 1860: 911-921, 2017.
36. Xie C, Mao X, Huang J, Ding Y, Wu J, Dong S, Kong L, Gao G, Li CY and Wei L: KOBAS 2.0: A web server for annotation and identification of enriched pathways and diseases. Nucleic Acids Res 39: W316-W322, 2011.
37. Young MD, Wakefield MJ, Smyth GK and Oshlack A: Gene ontology analysis for RNA-seq: Accounting for selection bias. Genome Biol 11: R14, 2010.
38. Bartha Á and Győrffy B: TNMplot.com: A web tool for the comparison of gene expression in normal, tumor and metastatic tissues. Int J Mol Sci 22: 2622, 2021.
39. Szász AM, Lánczky A, Nagy Á, Förster S, Hark K, Green JE, Boussioutas A, Busuttil R, Szabó A and Győrffy B: Cross-validation of survival associated biomarkers in gastric cancer using transcriptomic data of 1,065 patients. Oncotarget 7: 49322-49333, 2016.
40. Grill JI, Neumann J, Ofner A, Marschall MK, Zierahn H, Herbst A, Wolf E and Kolligs FT: Dro1/Ccdc80 inactivation promotes AOM/DSS-induced colorectal carcinogenesis and aggravates colitis by DSS in mice. Carcinogenesis 39: 1176-1184, 2018.
41. Liu M, Guo S and Stiles JK: The emerging role of CXCL10 in cancer (Review). Oncol Lett 2: 583-589, 2011.
42. Chen LH, Liao CY, Lai LC, Tsai MH and Chuang EY: Semaphorin 6A attenuates the migration capability of lung cancer cells via the NRF2/HMOX1 Axis. Sci Rep 9: 13302, 2019.
43. Mizuguchi Y, Specht S, Lunz JG, Isse K, Corbitt N, Takizawa T and Demetris AJ: SPRR2A enhances p53 deacetylation through HDAC1 and down regulates p21 promoter activity. BMC Mol Biol 13: 20, 2012.
44. Li TF, Zeng HJ, Shan Z, Ye RY, Cheang TY, Zhang YJ, Lu SH, Zhang Q, Shao N and Lin Y: Overexpression of kinesin superfamily members as prognostic biomarkers of breast cancer. Cancer Cell Int 20: 123, 2020.
45. Lee HW, Park YM, Lee SJ, Cho HJ, Kim DH, Lee JI, Kang MS, Seol HJ, Shim YM, Nam DH, *et al*: Alpha-smooth muscle actin (ACTA2) is required for metastatic potential of human lung adenocarcinoma. Clin Cancer Res 19: 5879-5889, 2013.
46. Nagano K, Imai S, Zhao X, Yamashita T, Yoshioka Y, Abe Y, Mukai Y, Kamada H, Nakagawa S, Tsutsumi Y and Tsunoda S: Identification and evaluation of metastasis-related proteins, oxysterol binding protein-like 5 and calumenin, in lung tumors. Int J Oncol 47: 195-203, 2015.
47. Mansour MR, He S, Li Z, Lobbardi R, Abraham BJ, Hug C, Rahman S, Leon TE, Kuang YY, Zimmerman MW, *et al*: JDP2: An oncogenic bZIP transcription factor in T cell acute lymphoblastic leukemia. J Exp Med 215: 1929-1945, 2018.
48. Cairns J, Fridley BL, Jenkins GD, Zhuang Y, Yu J and Wang L: Differential roles of ERRFI1 in EGFR and AKT pathway regulation affect cancer proliferation. EMBO Rep 19: e44767, 2018.
49. Li D, Liu S, Xu J, Chen L, Xu C, Chen F, Xu Z, Zhang Y, Xia S, Shao Y and Wang Y: Ferroptosis-related gene CHAC1 is a valid indicator for the poor prognosis of kidney renal clear cell carcinoma. J Cell Mol Med 25: 3610-3621, 2021.
50. Chiu M, Taurino G, Bianchi MG, Kilberg MS and Bussolati O: Asparagine synthetase in cancer: Beyond acute lymphoblastic leukemia. Front Oncol 9: 1480, 2019.
51. Du F, Sun L, Chu Y, Li T, Lei C, Wang X, Jiang M, Min Y, Lu Y, Zhao X, *et al*: DDIT4 promotes gastric cancer proliferation and tumorigenesis through the p53 and MAPK pathways. Cancer Commun (Lond) 38: 45, 2018.
52. Yin S, Chen F, Ye P and Yang G: Overexpression of FAM3C protein as a novel biomarker for epithelial-mesenchymal transition and poor outcome in gastric cancer. Int J Clin Exp Pathol 11: 4247-4256, 2018.
53. Chan YC, Chang YC, Chuang HH, Yang YC, Lin YF, Huang MS, Hsiao M, Yang CJ and Hua KT: Overexpression of PSAT1 promotes metastasis of lung adenocarcinoma by suppressing the IRF1-IFNγ axis. Oncogene 39: 2509-2522, 2020.
54. Rawat V, Malvi P, Della Manna D, Yang ES, Bugide S, Zhang X, Gupta R and Wajapeyee N: PSPH promotes melanoma growth and metastasis by metabolic deregulation-mediated transcriptional activation of NR4A1. Oncogene 40: 2448-2462, 2021.
55. Meng Q, Ren M, Li Y and Song X: LncRNA-RMRP Acts as an oncogene in lung cancer. PLoS One 11: e0164845, 2016.
56. Wang ET, Sandberg R, Luo S, Khrebtukova I, Zhang L, Mayr C, Kingsmore SF, Schroth GP and Burge CB: Alternative isoform regulation in human tissue transcriptomes. Nature 456: 470-476, 2008.
57. Duan Z, Zhang J, Choy E, Harmon D, Liu X, Nielsen P, Mankin H, Gray NS and Hornicek FJ: Systematic kinome shRNA screening identifies CDK11 (PITSLRE) kinase expression is critical for osteosarcoma cell growth and proliferation. Clin Cancer Res 18: 4580-4588, 2012.
58. Byun HJ, Kim BR, Yoo R, Park SY and Rho SB: sMEK1 enhances gemcitabine anti-cancer activity through inhibition of phosphorylation of Akt/mTOR. Apoptosis 17: 1095-1103, 2012.
59. Yang Q, Zhu M, Wang Z, Li H, Zhou W, Xiao X, Zhang B, Hu W and Liu J: 4.1N is involved in a flotillin-1/β-catenin/Wnt pathway and suppresses cell proliferation and migration in non-small cell lung cancer cell lines. Tumour Biol 37: 12713-12723, 2016.

60. Durinck S, Stawiski EW, Pavía-Jiménez A, Modrusan Z, Kapur P, Jaiswal BS, Zhang N, Toffessi-Tcheuyap V, Nguyen TT, Pahuja KB, *et al*: Spectrum of diverse genomic alterations Define non-clear cell renal carcinoma subtypes. Nat Genet 47: 13-21, 2015.
61. Starrett GJ, Luengas EM, McCann JL, Ebrahimi D, Temiz NA, Love RP, Feng Y, Adolph MB, Chelico L, Law EK, *et al*: The DNA cytosine deaminase APOBEC3H haplotype I likely contributes to breast and lung cancer mutagenesis. Nat Commun 7: 12918, 2016.
62. Lin D, Dong X, Wang K, Wyatt AW, Crea F, Xue H, Wang Y, Wu R, Bell RH, Haegert A, *et al*: Identification of DEK as a potential therapeutic target for neuroendocrine prostate cancer. Oncotarget 6: 1806-1820, 2015.
63. Datta A, Adelson ME, Mogilevkin Y, Mordechai E, Sidi AA and Trama JP: Oncoprotein DEK as a tissue and urinary biomarker for bladder cancer. BMC Cancer 11: 234, 2011.
64. Wise-Draper T, Sendilnathan A, Palackdharry S, Pease N, Qualtieri J, Butler R, Sadraei NH, Morris JC, Patil Y, Wilson K, *et al*: Decreased plasma DEK oncogene levels correlate with p16-Negative disease and advanced tumor stage in a case-control study of patients with head and neck squamous cell carcinoma. Transl Oncol 11: 168-174, 2018.
65. Biyik-Sit R, Kruer T, Dougherty S, Bradley JA, Wilkey DW, Merchant ML, Trent JO and Clem BF: Nuclear pyruvate kinase M2 (PKM2) contributes to phosphoserine aminotransferase 1 (PSAT1)-mediated cell migration in EGFR-activated lung cancer cells. Cancers (Basel) 13: 3938, 2021.
66. Ferraro A, Schepis F, Leone V, Federico A, Borbone E, Pallante P, Berlingieri MT, Chiappetta G, Monaco M, Palmieri D, *et al*: Tumor suppressor role of the CL2/DRO1/CCDC80 gene in thyroid carcinogenesis. J Clin Endocrinol Metab 98: 2834-2843, 2013.
67. De S, Cipriano R, Jackson MW and Stark GR: Overexpression of kinesins mediates docetaxel resistance in breast cancer cells. Cancer Res 69: 8035-8042, 2009.